Differential cross-section measurement of the $^{14}N(n, p)^{14}C$ reaction in the 0.1-6.0 MeV energy region

Wei Jiang, Qiuyue Luo, Ruirui Fan, Kang Sun, et al.

Institute of high energy physics, Chinese Academy of Sciences
Spallation Neutron Source Science Center

Content

Motivation and Background

$^{14}N(n, p)^{14}C$ reaction:

1. Understanding of cosmic-ray physics and nucleosynthesis.

2. The development and refinement of nuclear reaction theory models.

3. Neutron-based medical therapy.

Motivation and Background

- Wallner, et al (2016)： Suggest that the cross section of the resonance at 493 keV should be ~3.3 lower than Morgan's (1979) experimental results.
- Pablo Torres-Sánchez (2023)： With SAMMY fitting, the cross section at 493 keV is consistent with the ENDF/B-VIII.0 evaluations.
- Pablo Torres-Sánchez (2023)： The low-energy tail(100-480 keV) of the resonance at ~490 keV is lower than the ENDF/B-VIII.0 evaluation, where there are disagreements among existing experimental results.
- From 800 keV to 2.5 MeV, some resonances are present in the JENDL-5.0 but not in the ENDF/B-VIII.1.
- There is a lack of differential cross section for the $^{14}N(n, p)^{14}C$ reaction in the entire energy range.

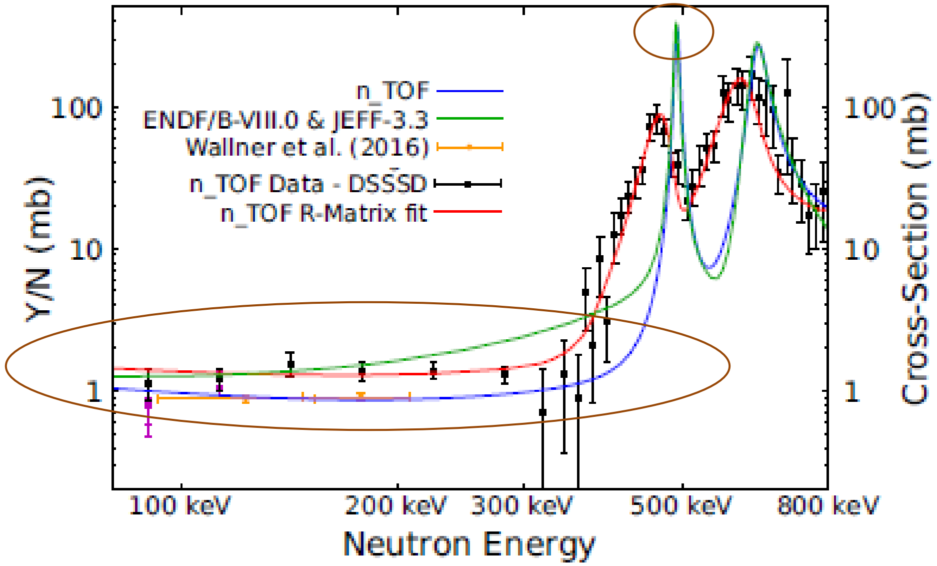

Get from PHYSICAL REVIEW C 107, 064617 (2023)

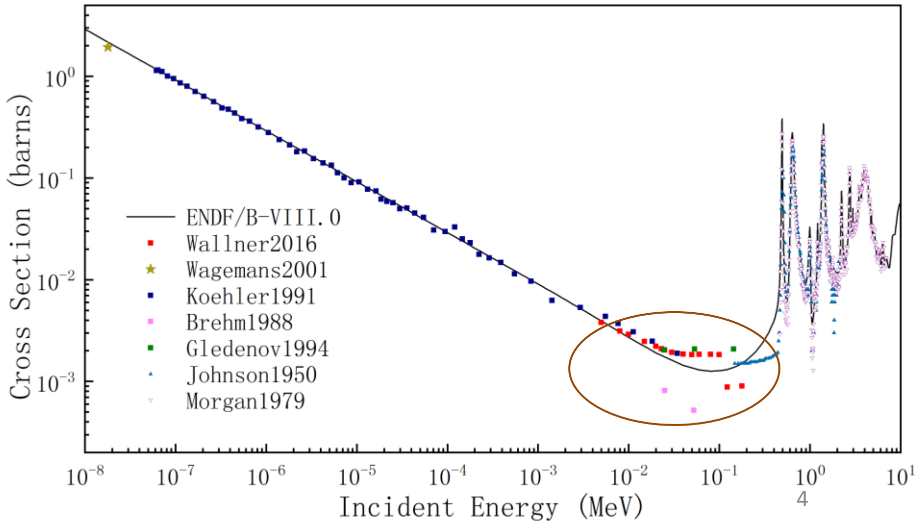

CSNS Back-n white neutron facility

- The China Spallation Neutron Source Back-n white neutron facility in DongGuan, south China.
- Pulse neutron beam; Energy range: 0.3 eV-300 MeV(with Gd absorber in the beamline)
- Time interval between two pulses: 40 ms (25 Hz)
- Double bunches; Pulse width: 60 ns (FWHM).

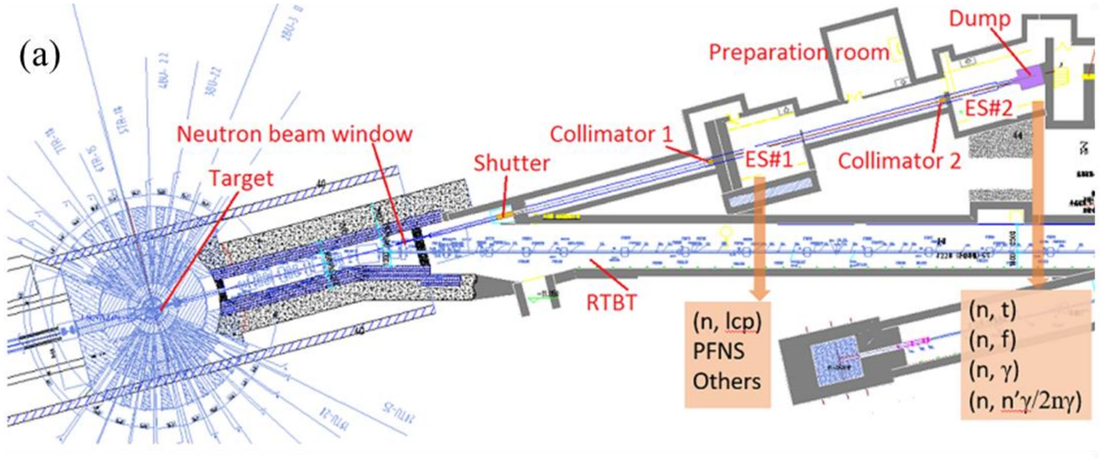

CSNS Back-n white neutron facility

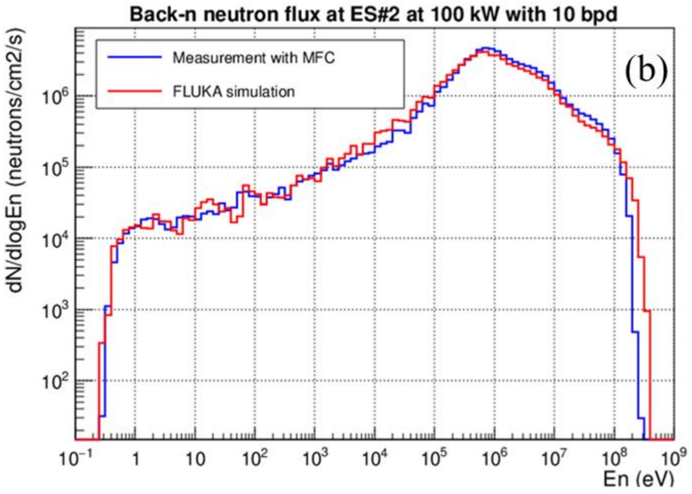

Back-n's energy spectrum

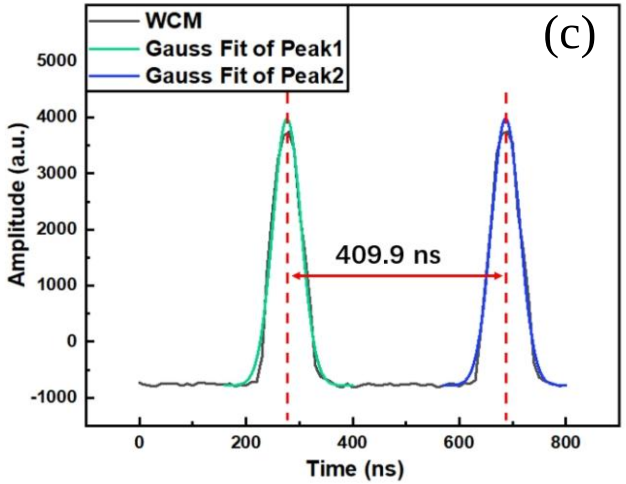

Double-bunch structure

Experimental Setup

- 13 Si-PIN detectors

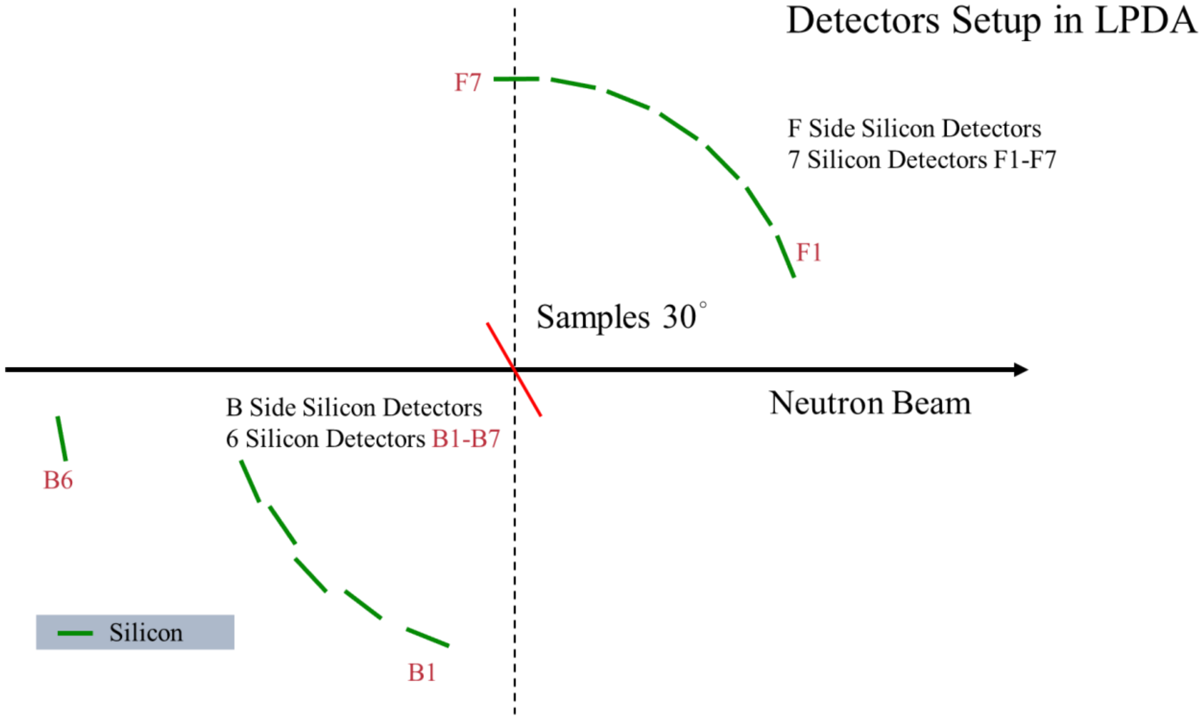

Beam spot's diameter at sample: ~14mm

Detector	F1	F2	F3	F4	F5	F6	F7
Angle(°)	21.4	32.86	44.29	55.71	67.14	78.57	90
D(mm)	189.5	189.5	189.5	189.5	189.5	189.5	189.5

B1	B2	B3	B4	B5	B6
105	121.32	133.88	146.41	158.74	170
193	195.61	202.73	193.75	204.64	360

Experiment Setup

- 1# $^{241}Am+^{244}Cm$： standard α source for energy calibration;
- 2# Al: 10.8 μm thick Al substrate for background measurement;
- 3# **$Al+C_3H_6N_6$**： Double-sided target, with a single side **$C_3H_6N_6$** of 200 μg/cm², deposited on a 10.8 μm Al substrate; Diameter 6 cm.

  (We also have tried BN target, but failed with the target.)

- 4# $Al+^{6}LiF$： Single-sided target, 360 μg/cm², deposited on a 10 μm Al substrate;
  - For reference measurement

2

3

4

Target thickness and uniformity measurement-$C_3H_6N_6$

Rutherford backscatter experiment

- Conducted at Peking University, 0.85 MeV protons
- Number/percentage of atoms of ^{14}N at 44 measurement points in both side of the target

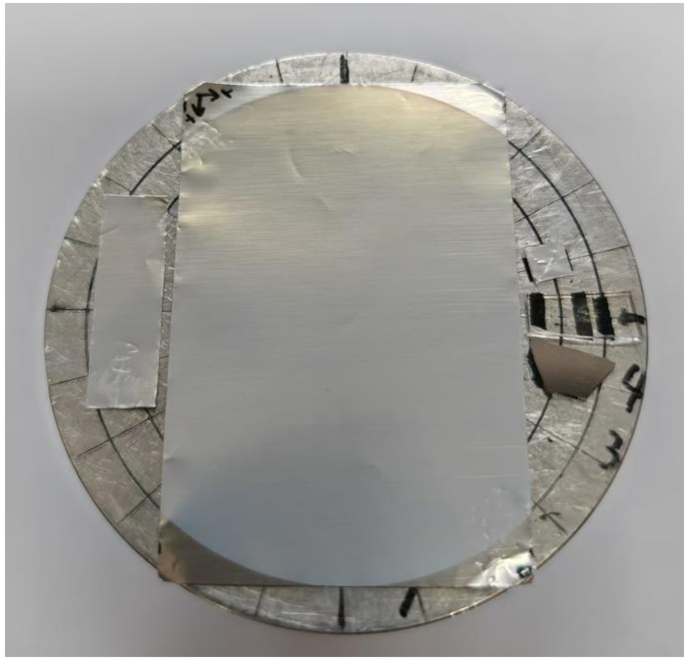

Sample for Rutherford backscatter
（Cropped $C_3H_6N_6$ target）

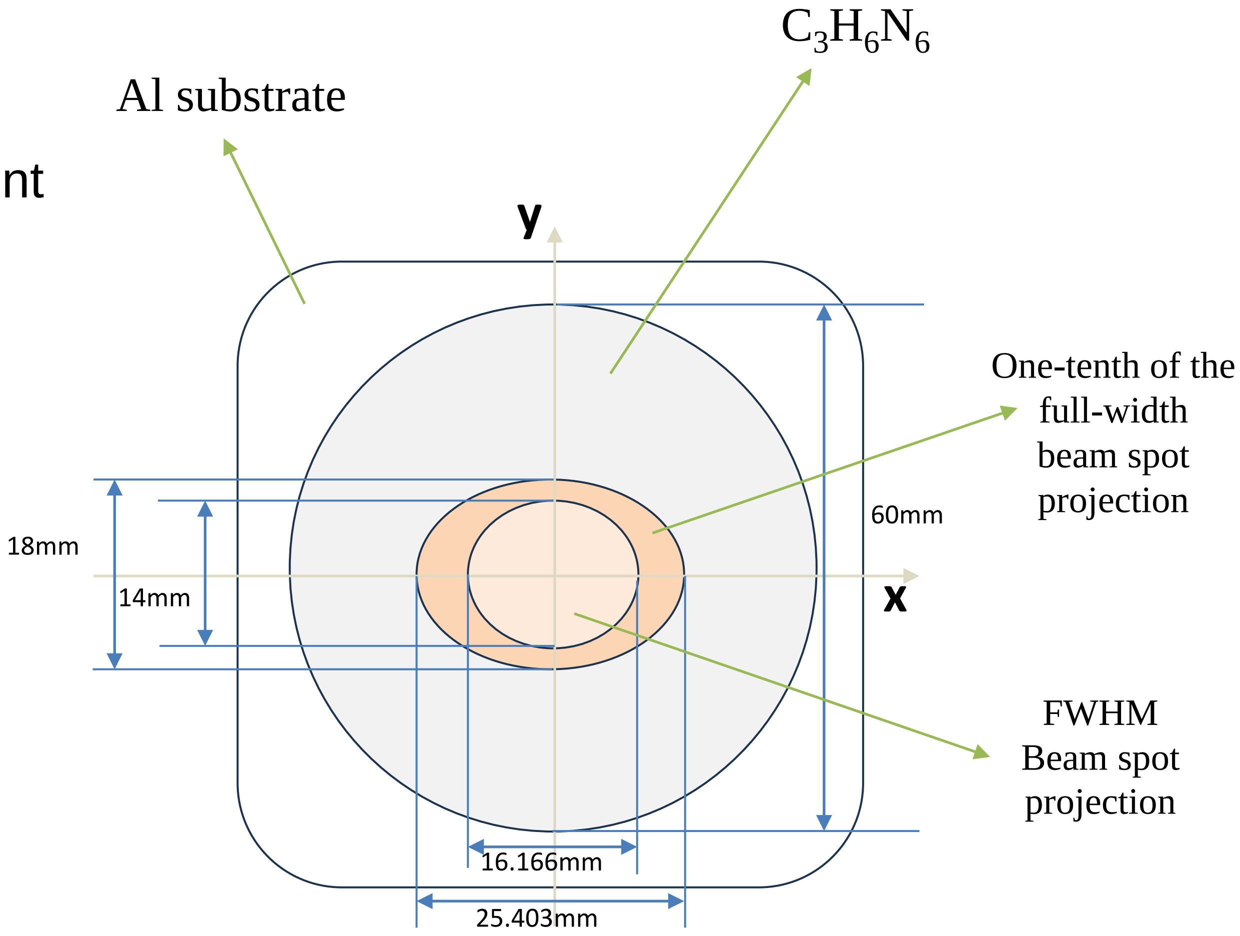

Schematic diagram of $C_3H_6N_6$ target

Target thickness and uniformity measurement-$C_3H_6N_6$

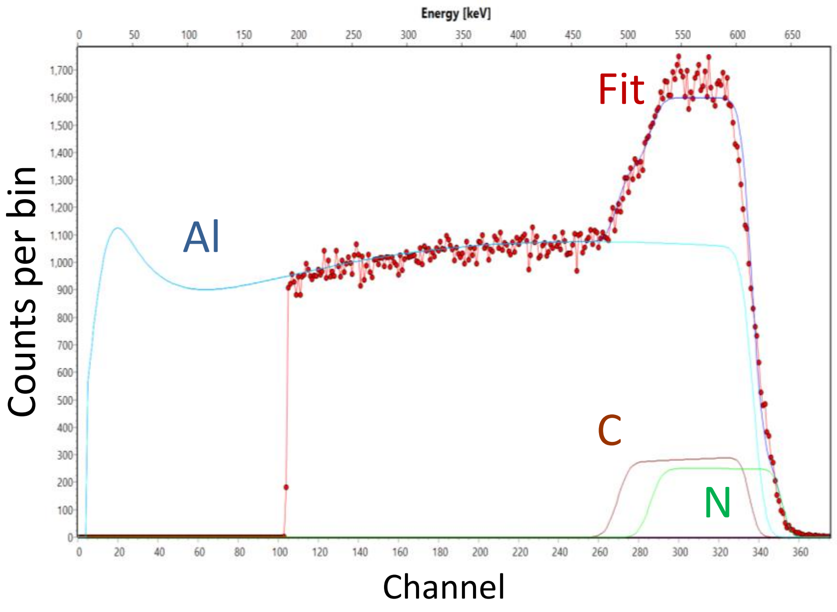

Rutherford backscatter energy spectra and SIMNRA fitting of each element at the measurement point

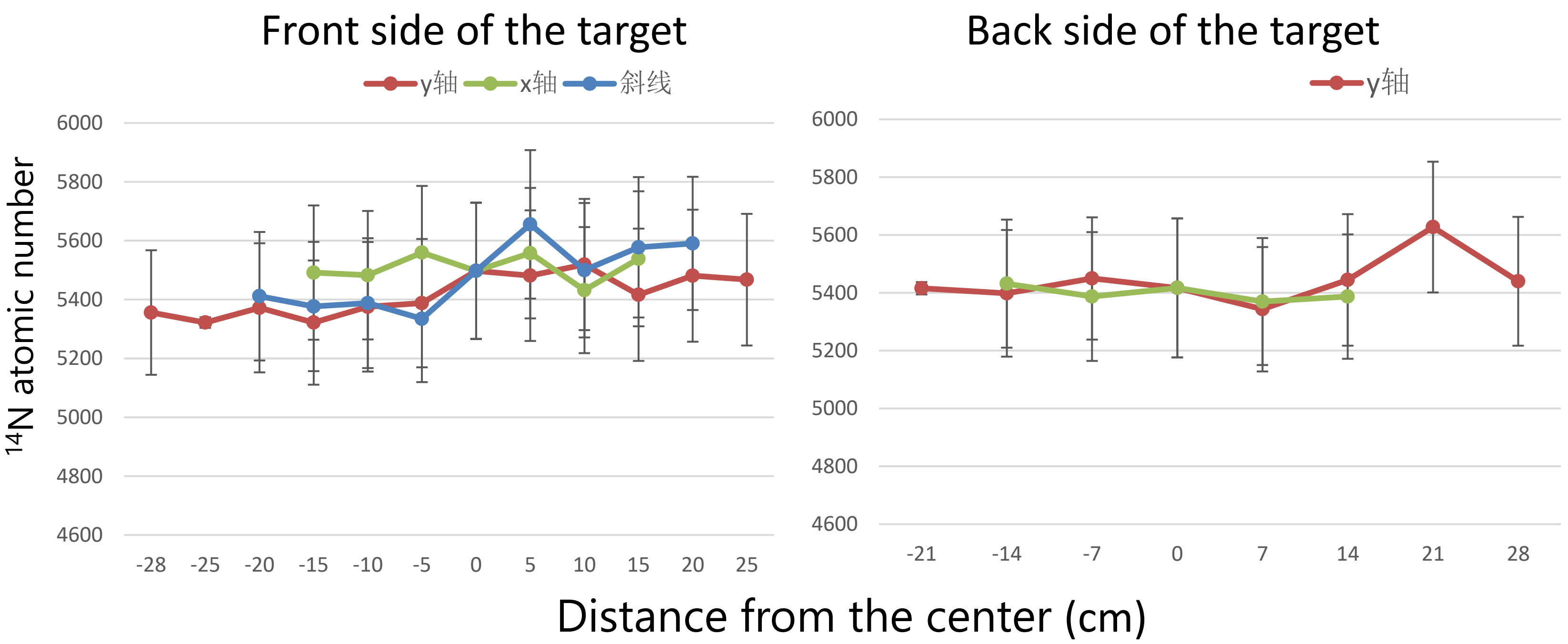

Fitted ^{14}N atomic number thickness (10^{15} atoms/cm^2)

	Atomic number thickness (10^{15} atoms/cm^2)	Proportion of ^{14}N atoms in $C_3H_6N_6$	^{14}N atomic number thickness (10^{15} atoms/cm^2)
Nominal	14300	0.4	5720
Front side	14377.68	0.38	5468.78 ± 43.08
Back side	14352.94	0.38	5416.88 ± 62.22

Conclusion: The $C_3H_6N_6$ target has good uniformity within uncertainty.

Data Processing

1# 2D spectra of Amplitude vs E_n

- Energy calibration
- TOF calibration

2# Double bunch unfolding

3# Subtracting the background

4# Selecting event

- Event count
- 1D histogram of count vs. neutron energy

5# Relative differential cross sections of $^{14}N(n, p)$

- Referring to the standard cross sections of $^{6}Li(n,t)$
- Uncertainty analysis

6# Fitting with Legendre polynomial

- Angular distribution of differential cross sections
- Angle-integrated cross sections

7# R-Matrix Fitting

Double Bunch Unfolding

- Double bunch: the events outlined in **red** are produced from the first bunch while the ones in **green** are from the second bunch.

- Al+$C_3H_6N_6$： **Double-sided** target

* With TOF calibration already done

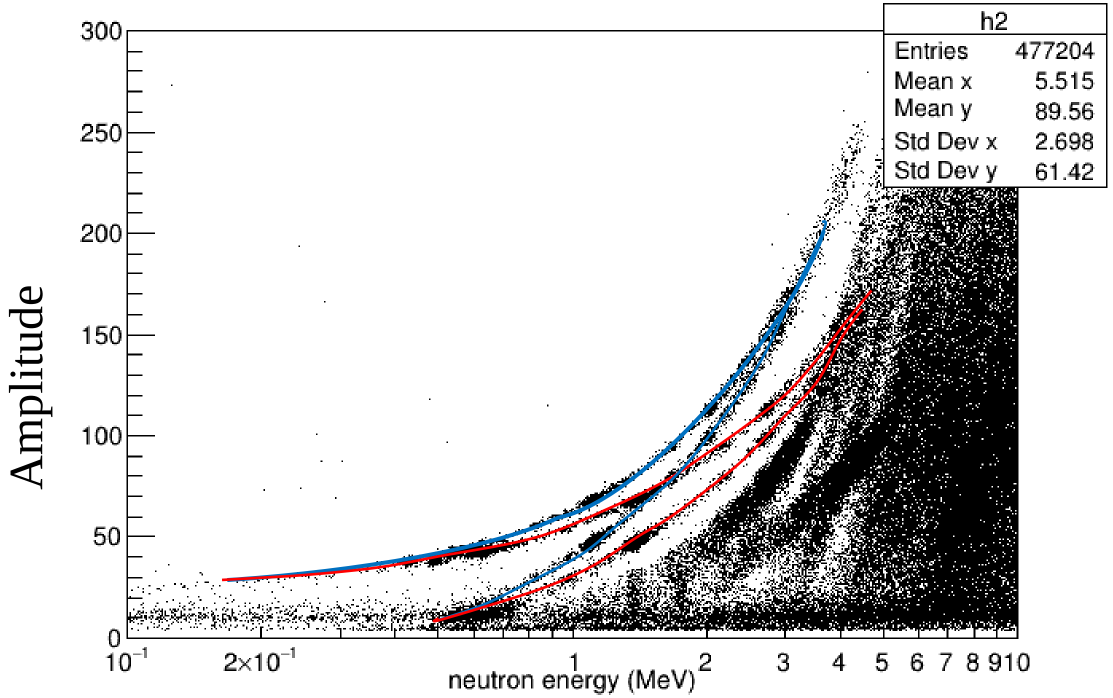

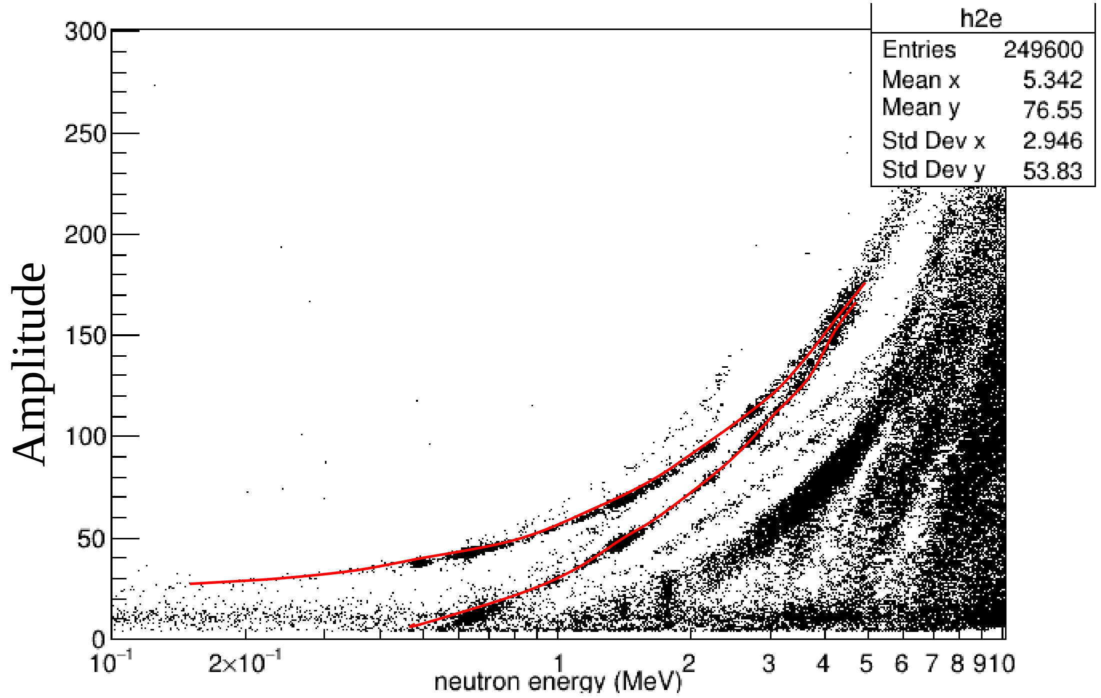

Amplitude vs E_n spectrum（133.88°）

Before unfolding

After unfolding

Counts of selected events ($^{14}N(n, p)^{14}C$)

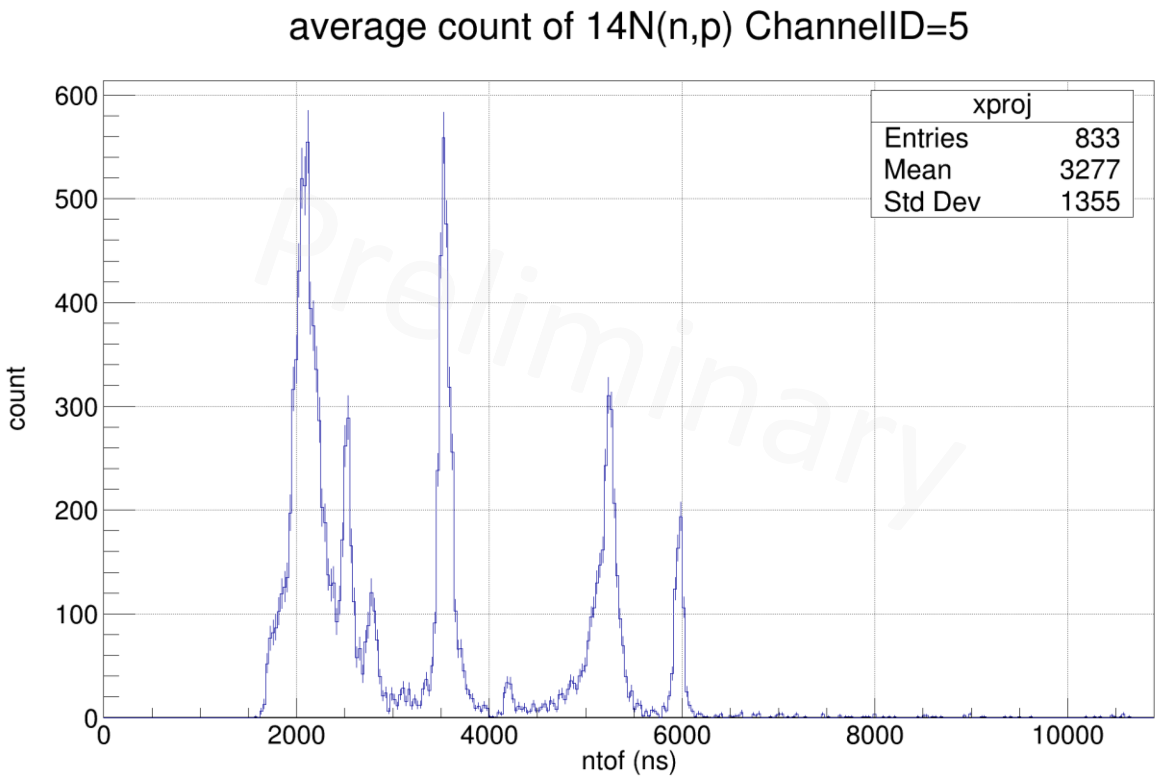

(*The background from Al has been subtracted)

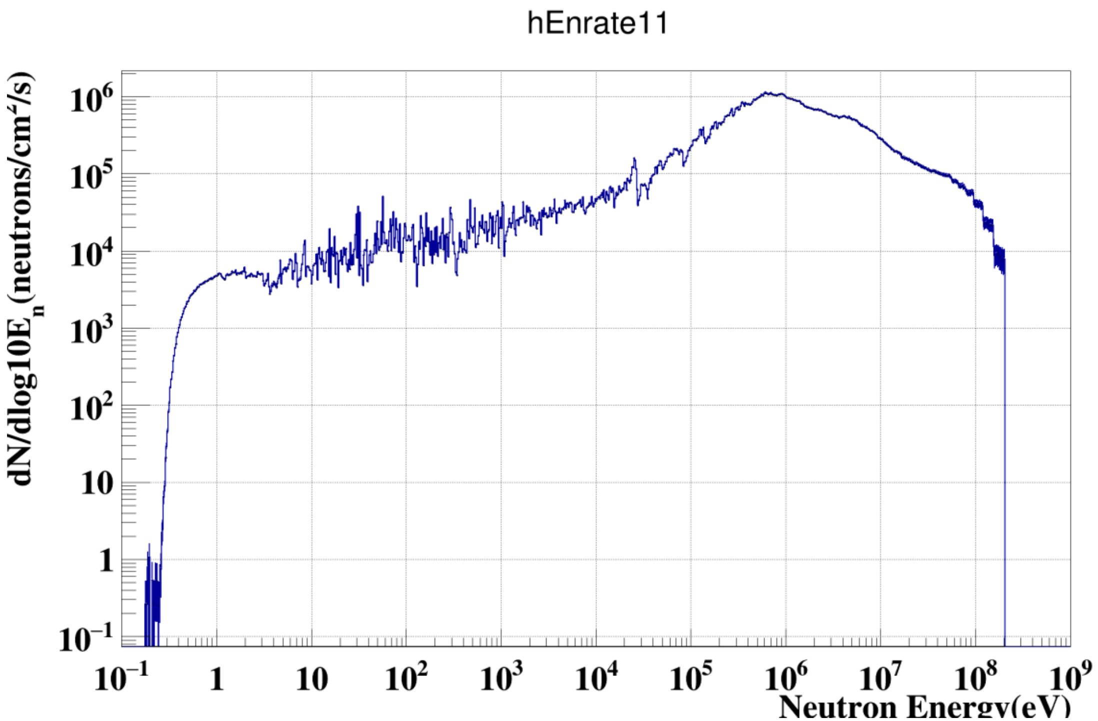

The energy spectrum of Back-n ES#1

When TOF of neutron is longer than ~3800 ns (E_n lower than ~1.3 MeV), the protons are only from the side facing forward.

Cross sections calculation

$$\frac{d\sigma}{d\Omega}\Big|_{E_n} = \frac{count(E_n)}{N_n(E_n)\cdot N_{target}\cdot \Omega_{\det}\cdot \epsilon_{\det}} = \mathrm{k}_{\det}\cdot\frac{count(E_n)}{N_n(E_n)\cdot N_{target}} \qquad (1)$$

- $count(E_n)$: count of proton at E_n
- $N_n(E_n)$: the number of the incident neutrons whose energy is equal to E_n, $\propto \mathrm{flux}_{E_n} \times \mathrm{proton}(t)$
- N_{target}: the number of target nuclei
- $\Omega_{\det}$, $\epsilon_{\det}$: the solid angle and the detecting efficiency of the detectors

- The cross section of ^{6}Li(n, t)α is standard and isotropic.
- The relative differential cross section of ^{14}N(n, p)^{14}C "normalization coefficient"

$$\frac{d\sigma}{d\Omega}(n14)\Big|_{E_n} = \frac{\mathrm{k}_{N14}}{\mathrm{k}_{Li6}}\cdot\frac{count(n14)_{E_n}}{\mathrm{flux}_{E_n}} \times \underbrace{\frac{d\sigma}{d\Omega}(Li6)\Big|_{E_i}}_{\text{from dataset}} \Big/ \underbrace{\frac{count(Li)_{E_i}}{\mathrm{flux}_{E_i}}}_{\text{measurement of } ^{6}\text{Li(n, t)}\alpha} \qquad (2)$$

- $\frac{\mathrm{k}_{N14}}{\mathrm{k}_{Li6}} = \frac{Nproton(^{6}\mathrm{LiF})}{Nproton(^{14}\mathrm{N})} \times \frac{Ntarget(^{6}\mathrm{Li})}{Ntarget(^{14}\mathrm{N})}$

Cross sections of $^{6}Li(n, t)^{4}He$

- For differential cross section (measurement):
  - Fit it with Legendre Polynomials

$$\frac{d\sigma}{d\Omega}(E, \cos\theta)$$

$$= \frac{\sigma_{n,x}(E)}{4\pi} \sum_{l=0}^{L} (2l+1) f_l(E) P_l(\cos\theta)$$

$$= \sum_{l=0}^{L} A_l P_l(\cos\theta) \qquad (3)$$

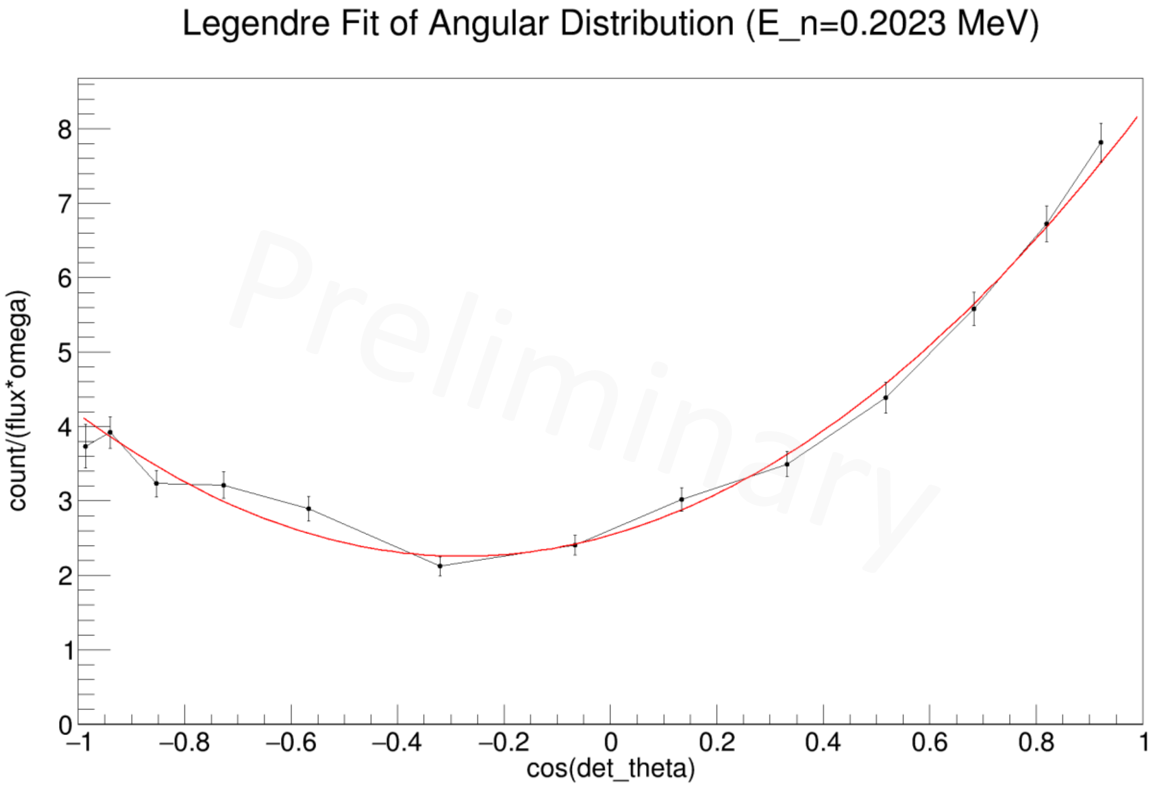

- For cross-section (unnormalized)
  - Integrate the fitting Legendre Polynomials along $\cos(det\_theta)$
  - Integral: $\sigma_{n,x}(E) = \int_{-1}^{1} 2\pi \frac{d\sigma}{d\Omega}(E, \cos\theta) \mathrm{d}\cos\theta \quad (4)$

The differential cross sections of $^{14}N(n, p)^{14}C$

- Range of neutron energy:

  ~50 keV— ~6.0 MeV

- Resonance at 0.491 ± 0.005 MeV
  - JENDL-5.0：0.4927 MeV
  - ENDF/B-VIII.1：0.491 MeV

- Resonance at 0.6344 ± 0.0075 MeV
  - JEDNL-5.0: 0.6351 MeV
  - ENDF/B-VIII.1 : 0.635 MeV

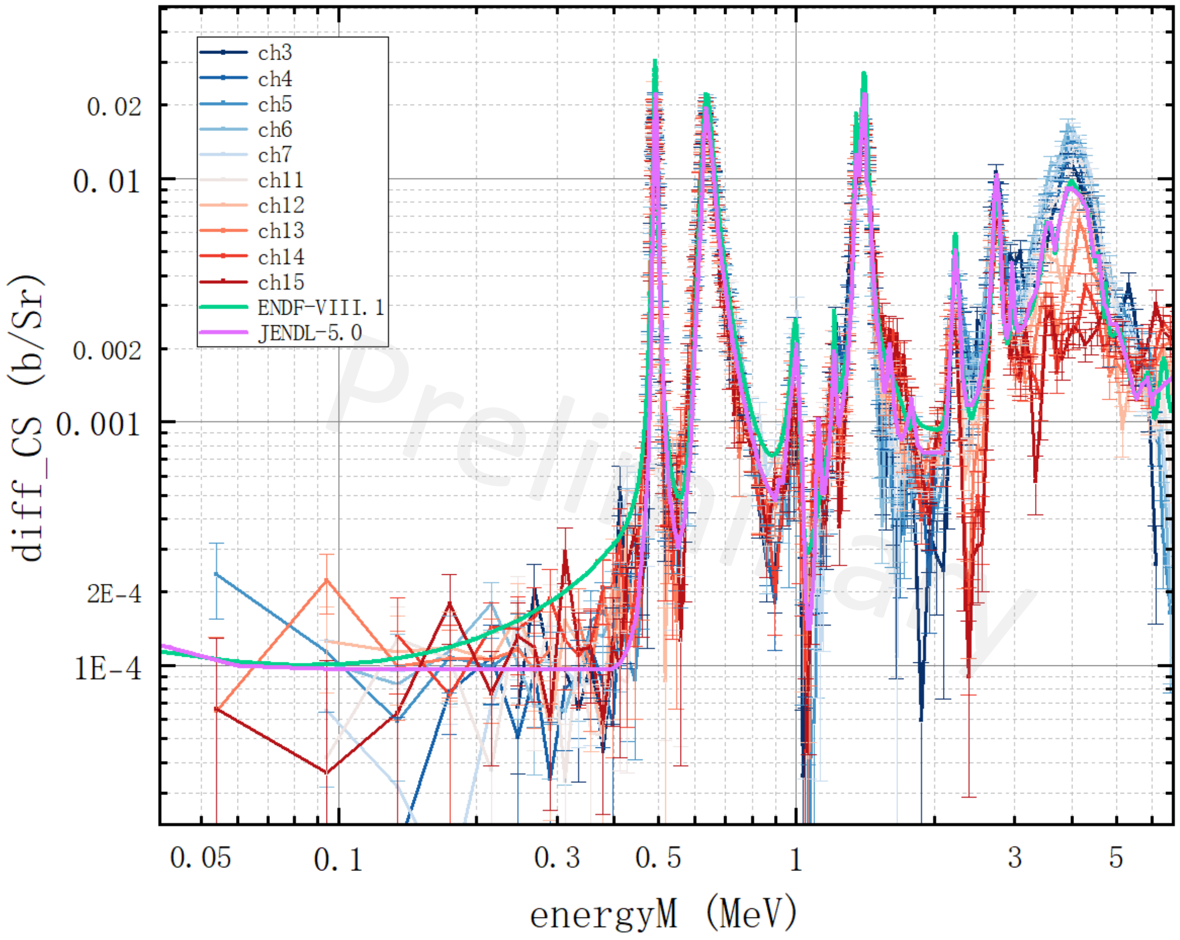

* in LAB frame

The differential cross sections of $^{14}N(n, p)^{14}C$

- Angular distribution of the measured differential cross section :
  - 2.2~2.8 MeV, 3~5 MeV
  - the total momentum of ^{15}N excited states: $J > \frac{3}{2}$
- Contribute to evaluation J and π of excited states

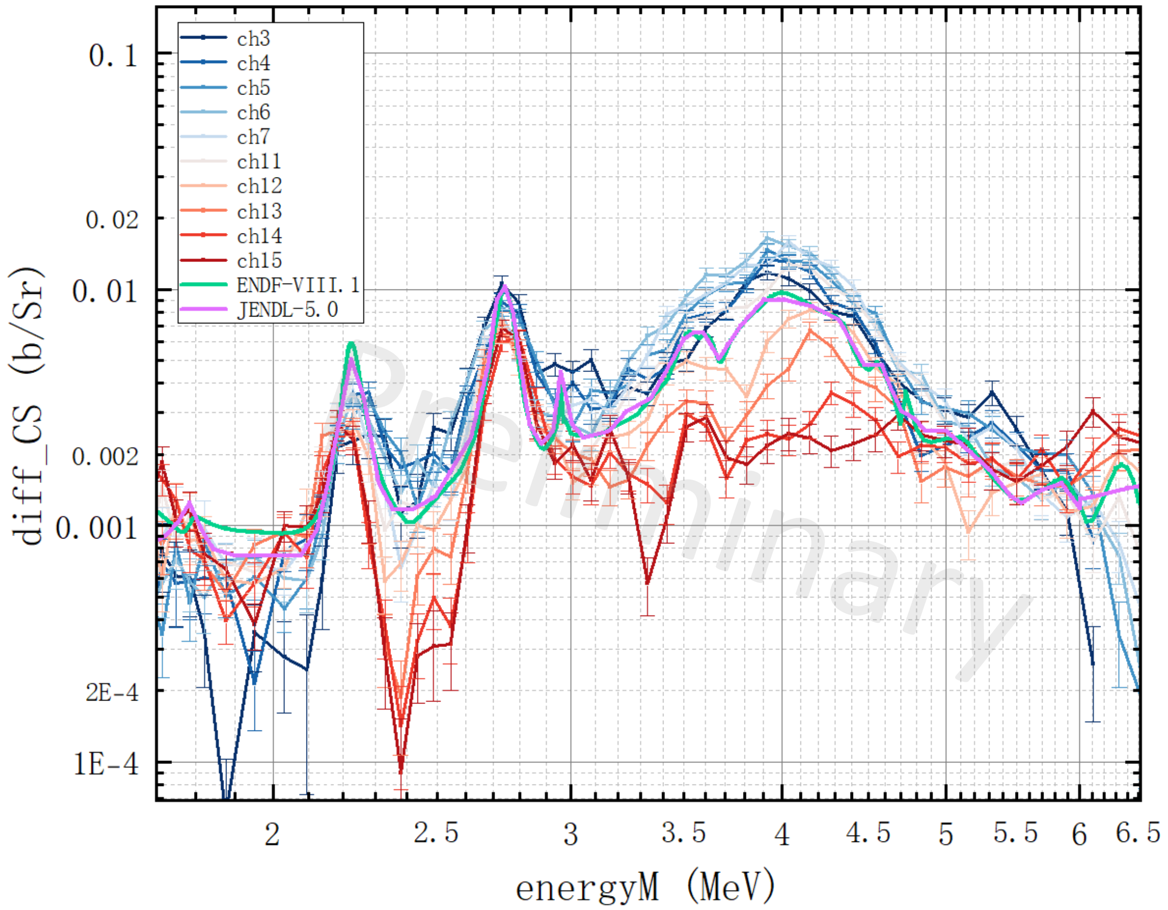

* in LAB frame

Fitting with Legendre Polynomials——Angular Distribution

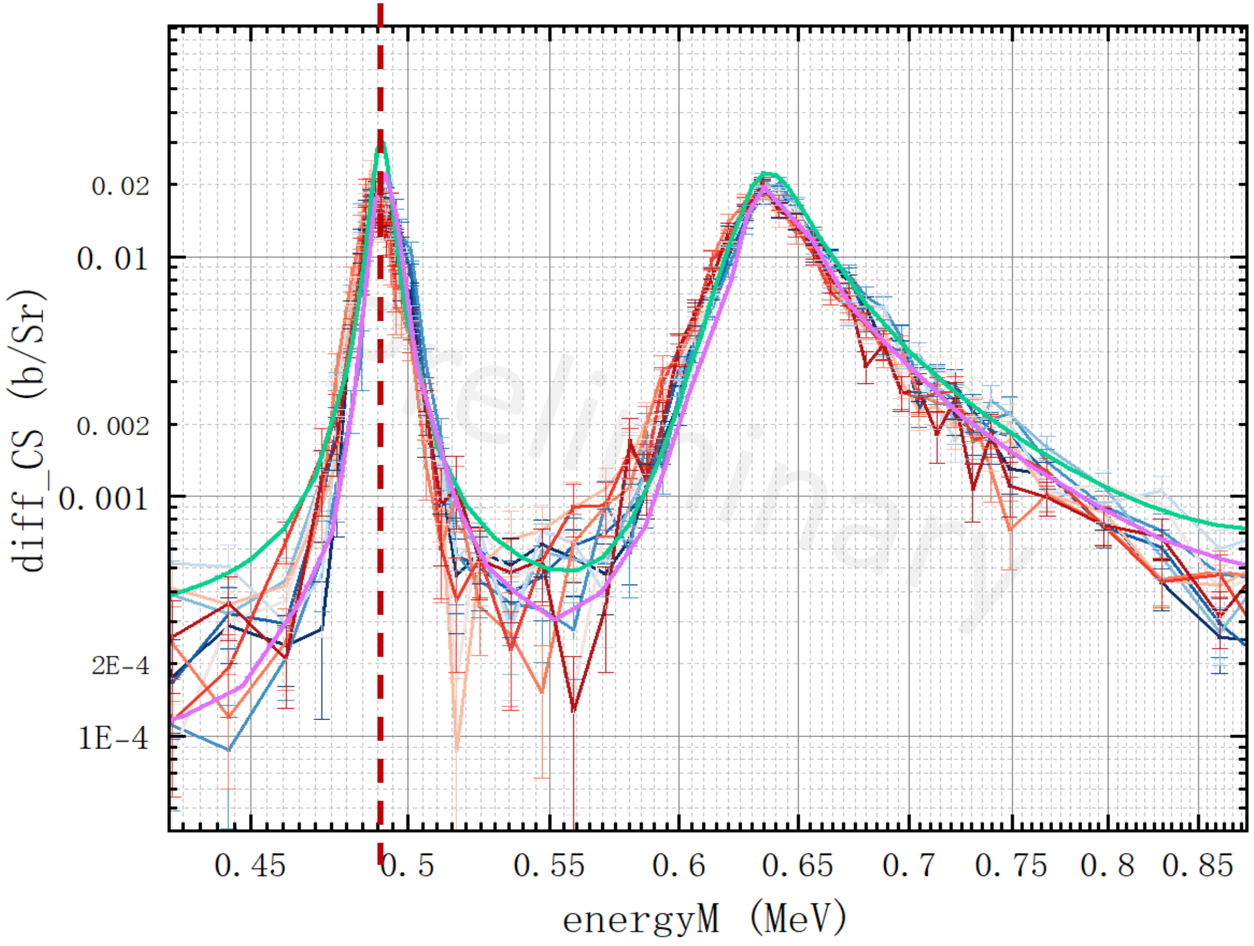

Differential cross sections of $^{14}N(n, p)$

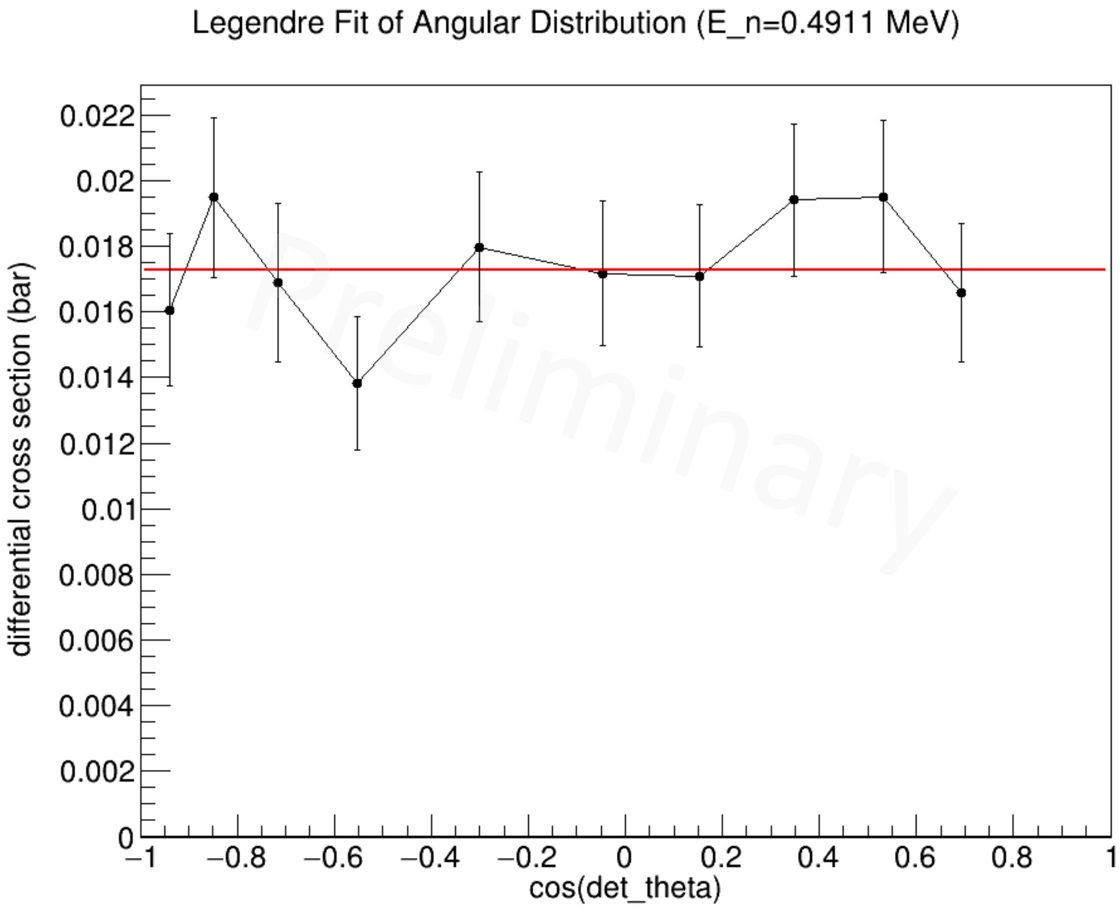

Angular distribution of differential cross sections (0.491MeV)

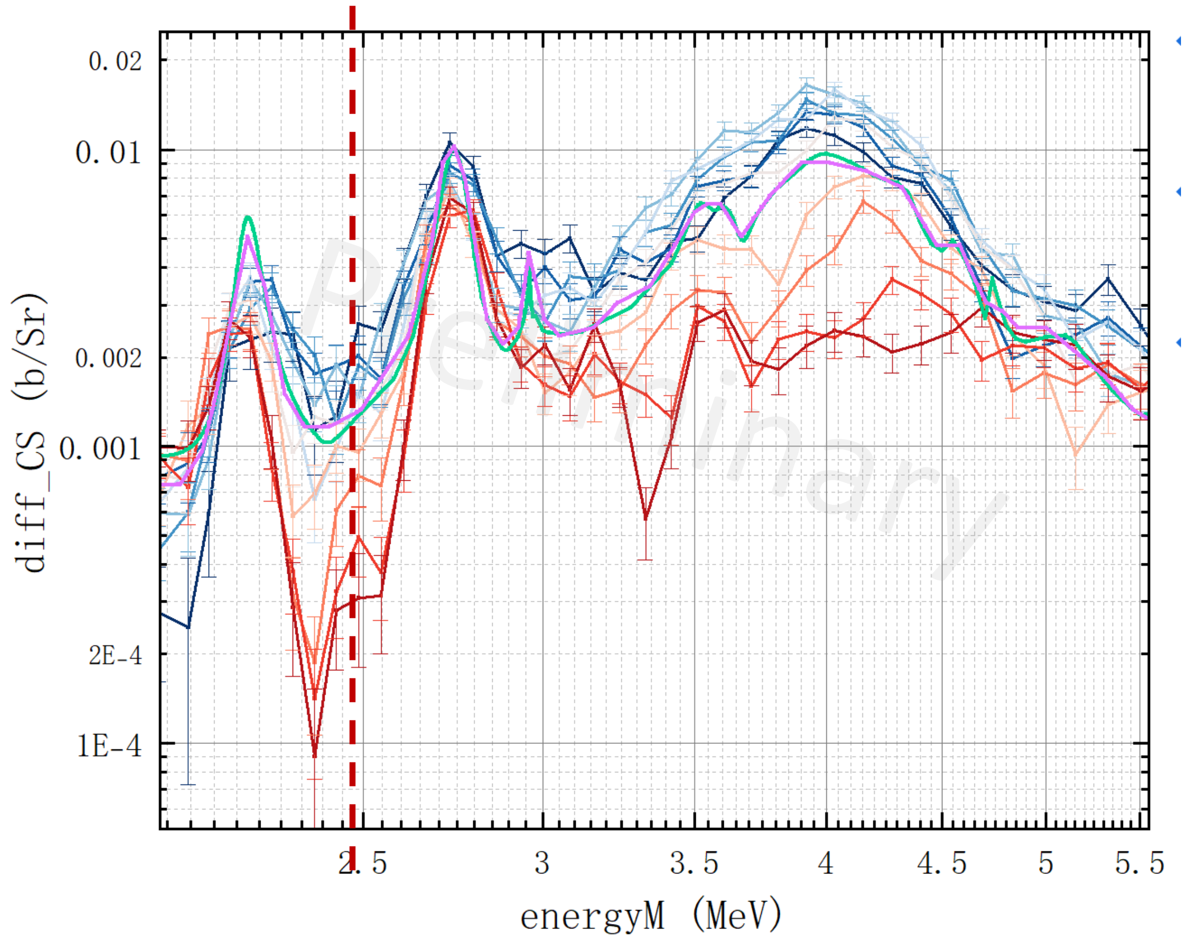

Differential cross sections of $^{14}N(n,p)$

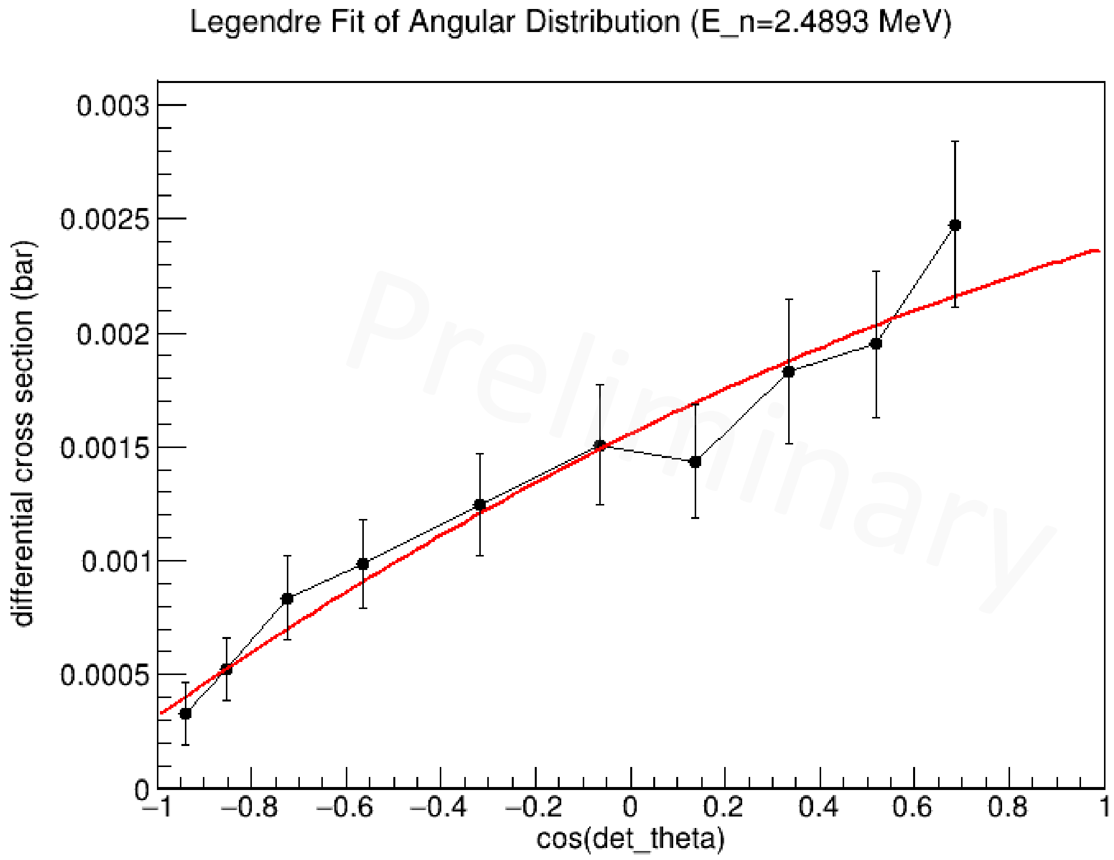

Angular distribution of differential cross sections (2.4893MeV)

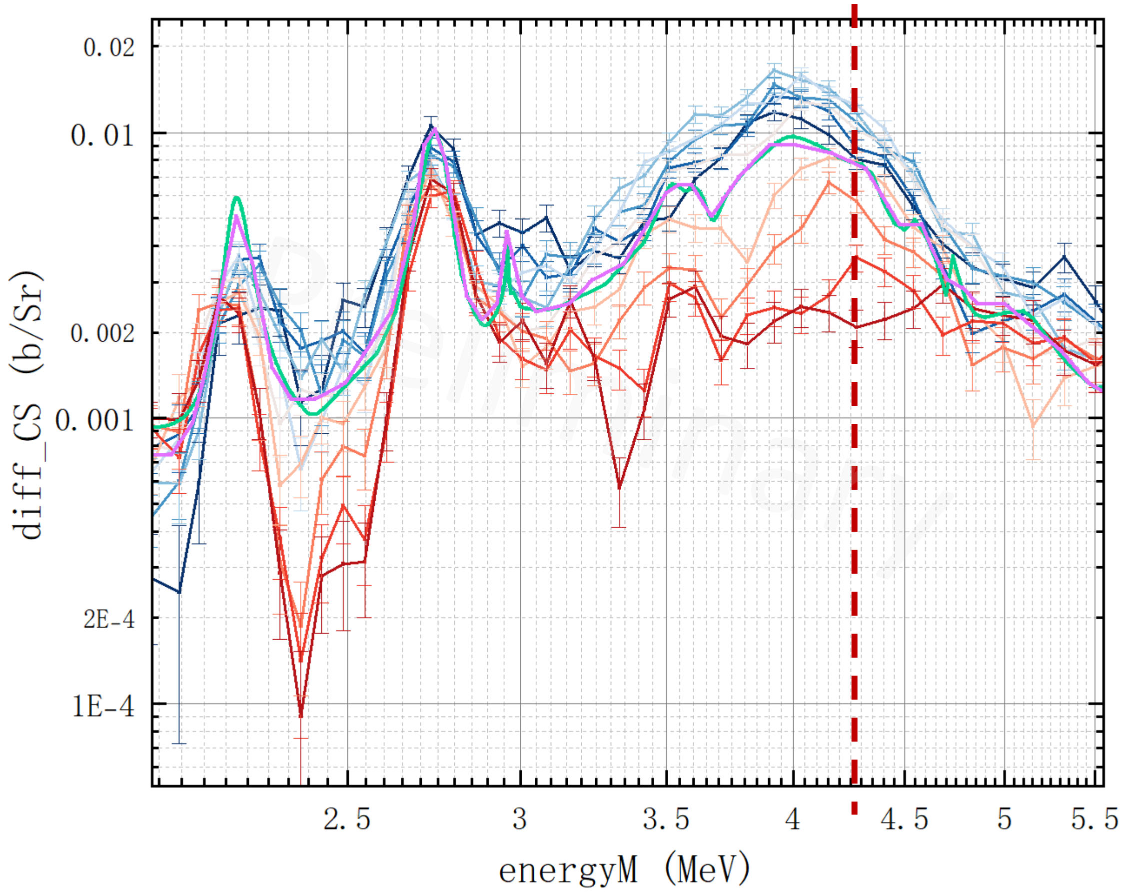

Differential cross sections of $^{14}N(n, p)$

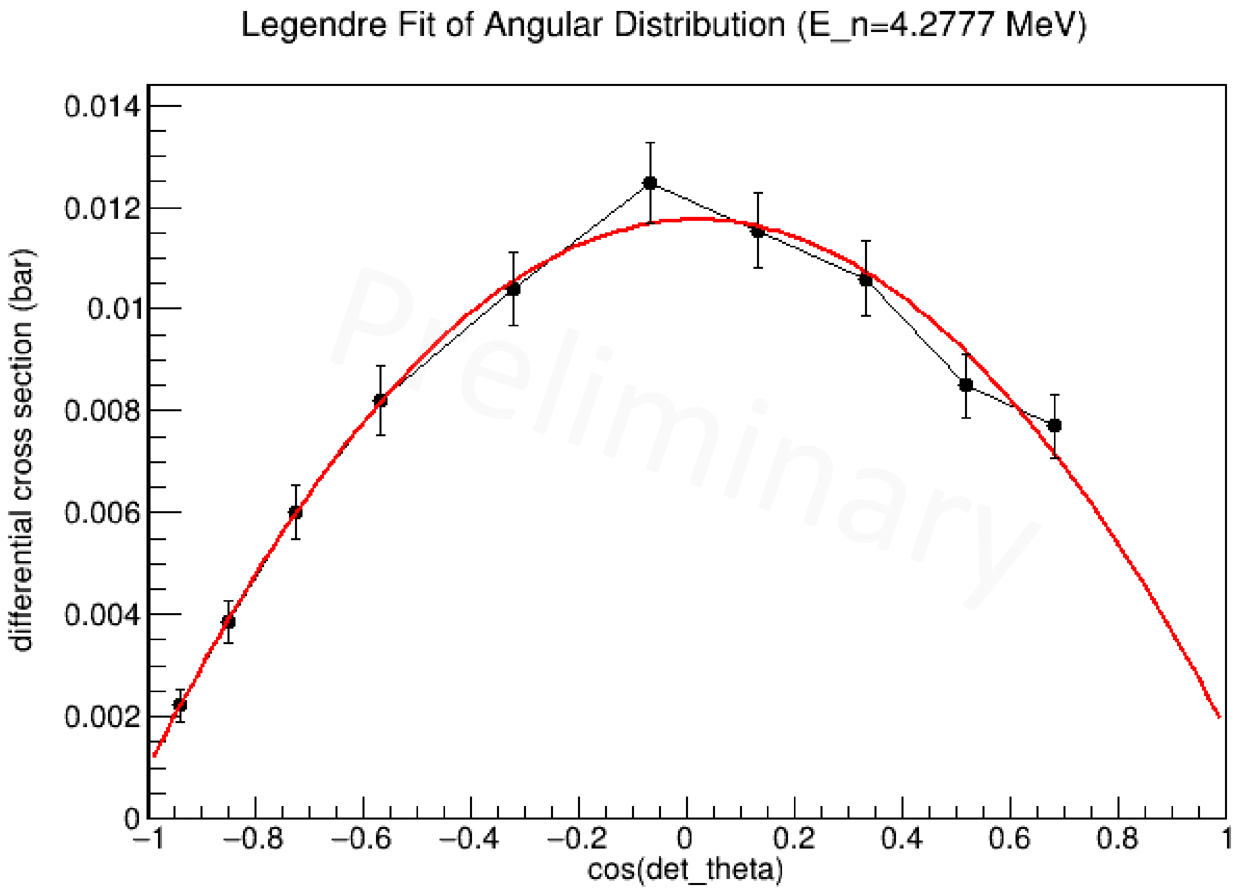

Angular distribution of differential cross sections (4.2777MeV)

Angle-integrated cross sections

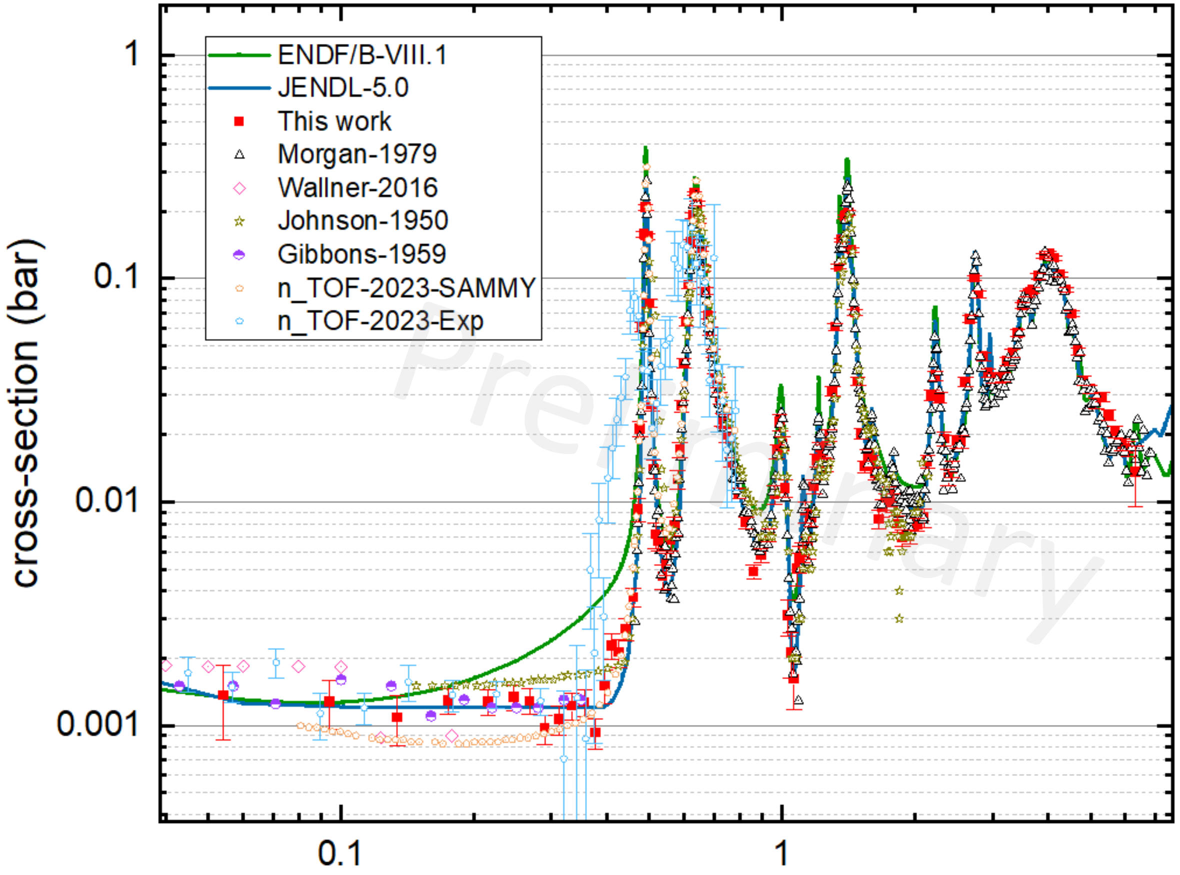

- E_n : 0.05-6 MeV
- Angle-integrated
- Uncertainty of cross sections: <5% at resonance

Angle-integrated cross section

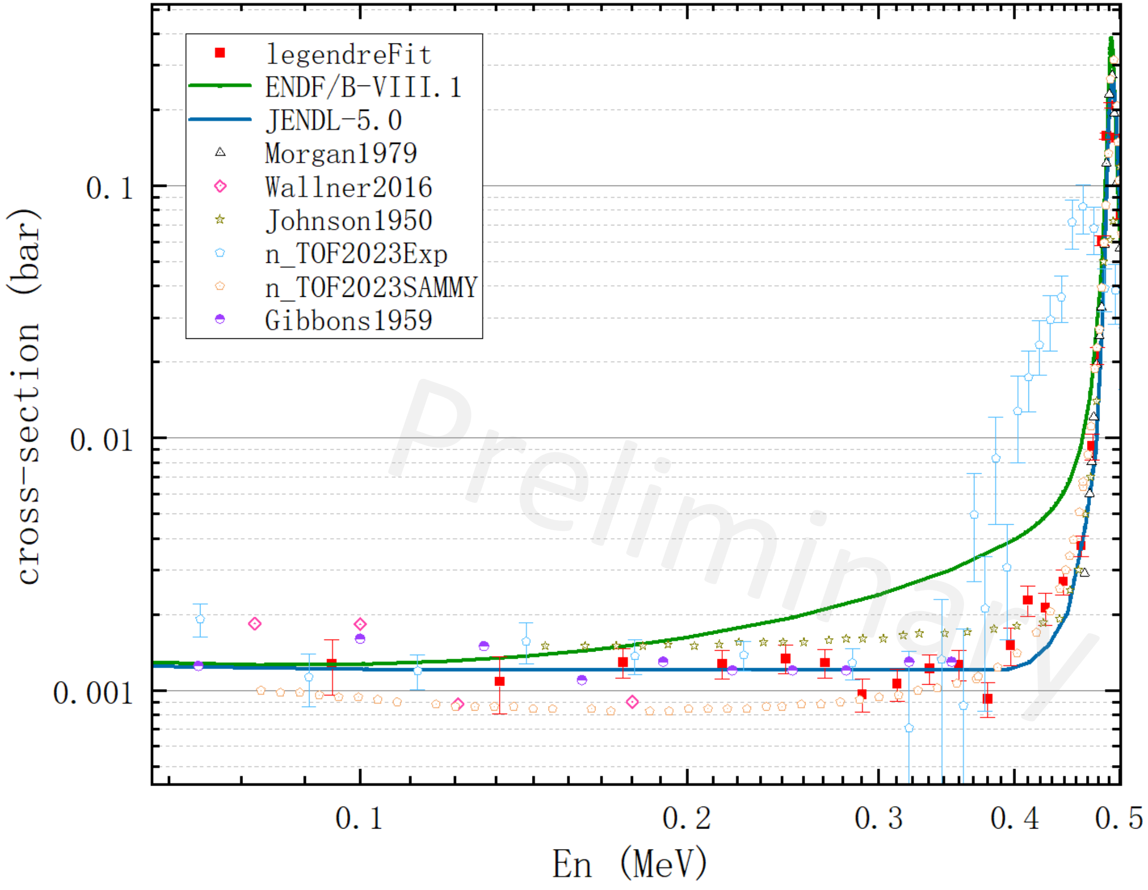

Cross sections in the 0.05-0.47 MeV(tail of the first resonance)

- Our results of the tail agree with the JENDL-5.0;
- The cross sections in the 0.05-0.35 MeV range support Gibbons(1959);
- The cross sections in the 0.4-0.47 MeV range support Johnson(1950) and the R-matrix(SAMMY) analysis of Pablo Torres-Sánchez (2023), and JENDL-5.0;
- A little higher than Wallner(2016) at 0.1-0.2 MeV;

Angle-integrated cross section

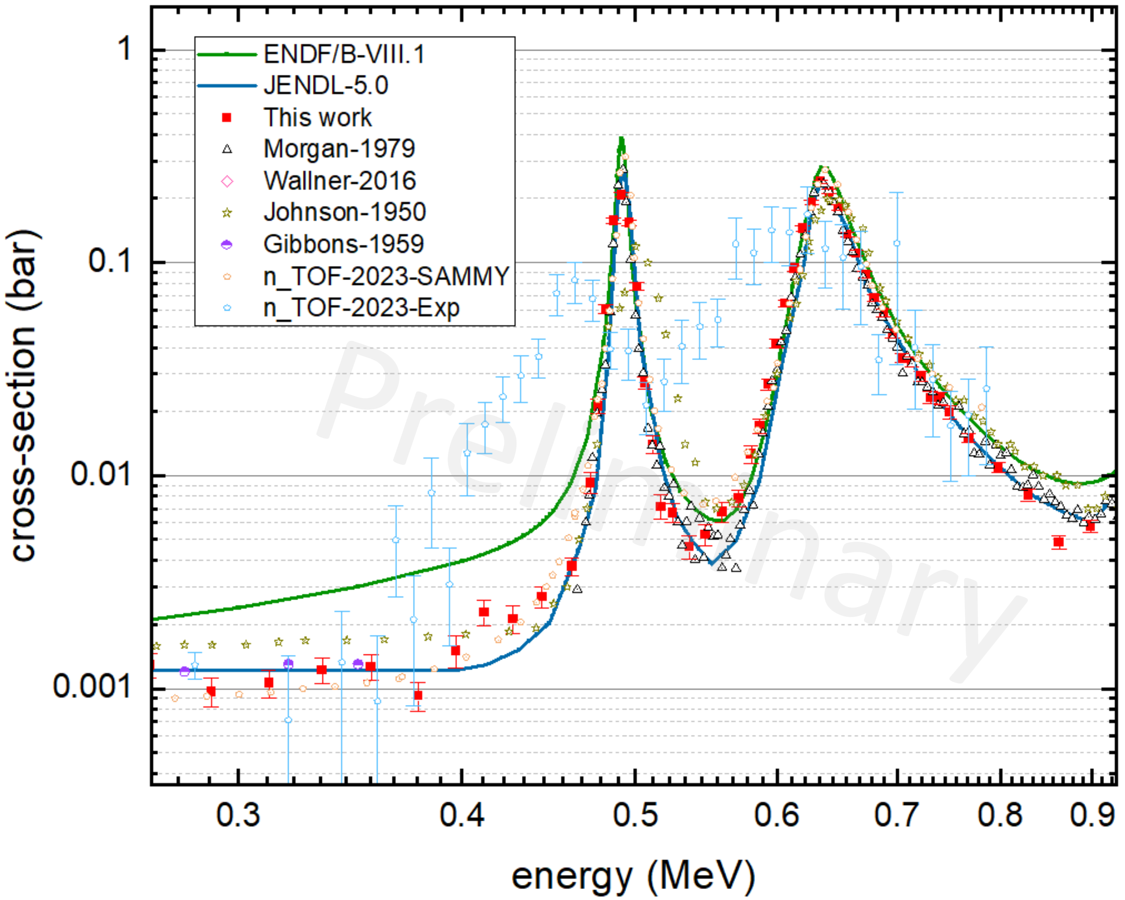

	Energy (MeV)	Cross section (barn)
This work	~0.4911 ± 0.0051	0.2079 ± 0.0055
JENDL-5.0	0.4927	**0.27744**
ENDF/B-VIII.1	0.491	**0.382958**
Morgan	~0.492	**~0.2739**

About half of the evaluation of ENDF/B-VIII.1.
Lower(about 3/4) than Morgan(1979)'s results.
Wallner(2016) suggested ~3.3 lower than Morgan(1979)'s results.

	Energy (MeV)	Cross section (barn)
This work	~0.6344 ± 0.0075	0.2399 ± 0.0051
JENDL-5.0	0.6351	0.244517
ENDF/B-VIII.1	0.635	0.279083

Agree with the JENDL-5.0.

SUMMARY

- Differential and angle-integrated cross sections of $^{14}N(n, p)^{14}C$ reaction are measured at the CSNS Back-n white neutron facility.
- The angle-integrated cross sections mostly agrees with the evaluations of the databases.
- In 0.05~0.45 MeV, the measured result agrees better with the evaluation of JENDL-5.0.
- The measured result at ~0.491 MeV is lower than the evaluation of JENDL-5.0 and lower than that of ENDF/B-VIII.1; The measured result at ~0.634 MeV agrees with the evaluation, within the measurement uncertainty.

Thanks for your attention!